

Low-temperature optical absorption in $\text{Al}_x\text{Ga}_{1-x}\text{As}$ grown by molecular-beam epitaxy

P. J. Pearch, W. T. Masselink, J. Klem, T. Henderson, and H. Morkoç

*Department of Electrical and Computer Engineering, Coordinated Science Laboratory, University of Illinois,
1101 W. Springfield Avenue, Urbana, Illinois 61801*

C. W. Litton and D. C. Reynolds

*U.S. Air Force Wright Aeronautical Laboratories, Avionics Laboratory (AFWAL/AADR),
Wright Patterson Air Force Base, Ohio 45433*

(Received 10 December 1984; revised manuscript received 26 April 1985)

A detailed study of optical absorption in the $\text{Al}_x\text{Ga}_{1-x}\text{As}$ alloy system is undertaken using optical transmission and photoluminescence data obtained at 3 K from molecular-beam epitaxial layers. Absorption coefficient spectra are calculated for the entire alloy composition range $0 \leq x \leq 1$. The first experimental data concerning AIAs in the region of the $\Gamma_{15V}-\Gamma_{1C}$ band gap are presented. The compositional dependence of threshold values of the absorption coefficient agrees with current theoretical predictions. Detailed excitonic structure is observed for the first time in the absorption spectra of $\text{Al}_x\text{Ga}_{1-x}\text{As}$ epilayers with $x \leq 0.43$. From this structure, free-exciton binding energies are determined. These energies display an x dependence qualitatively similar to that observed in donor activation energies in n -type $\text{Al}_x\text{Ga}_{1-x}\text{As}$.

INTRODUCTION

The $\text{GaAs}/\text{Al}_x\text{Ga}_{1-x}\text{As}$ compound semiconductor system has found application in a host of optoelectronic devices in recent years, including light-emitting diodes (LED's),¹ lasers,² and photodiodes.³ Yet despite the fundamental importance of this ternary alloy system to semiconductor science, little has been reported concerning optical absorption, especially in recent years. There is in particular a scarcity of data concerning AIAs. Previous studies have presented either extrapolated curves⁴ or have concentrated on spectral features near the indirect band gap.⁵ Also, due to absorption sample preparation techniques used in the past, most studies do not include data for low mole fraction layers ($x=0.3$), as etch selectivity thresholds are often in this range. This paper presents a complete study of optical absorption in the $\text{Al}_x\text{Ga}_{1-x}\text{As}$ alloy system over the entire composition range $0 \leq x \leq 1$ using photoluminescence and optical transmission data. Recent improvements in the state-of-the-art have permitted the growth of high-purity direct band-gap $\text{Al}_x\text{Ga}_{1-x}\text{As}$ epilayers exhibiting excitonic structure in the absorption spectra similar to that observed in GaAs. To the authors' knowledge, this constitutes the first report of detailed excitonic structure in $\text{Al}_x\text{Ga}_{1-x}\text{As}$ absorption spectra. At the opposite end of the composition range, results from the first application of this technique to directly determine experimentally the absorption coefficient of AIAs far above the indirect band gap are reported.

EXPERIMENTAL

The epilayers involved in this study were grown by molecular-beam epitaxy (MBE) on [100] GaAs substrates, the preparation of which has been discussed elsewhere.⁶ An arsenic cracker⁷ was used to produce an As_2 molecular

flux. Aluminum arsenide mole fractions (x) in the direct-band-gap region were determined from optical measurements, while those in the indirect region were estimated from growth rates and absorption data. Thicknesses were measured with a scanning electron microscope (SEM), using samples cleaved from areas of the wafers adjacent to the respective absorption samples. These thicknesses, all of which fall between 1.0 and 3.0 μm , are expected to be quite accurate, as a rotating substrate manipulator was employed during epitaxial growth, thus ensuring epilayer uniformity. Layers with low Al content ($x \leq 0.39$) and the AIAs layer were not intentionally doped, and are typically p type with carrier concentrations estimated to be in the 10^{15}-cm^{-3} range at 300 K, increasing with x . The background impurity level in GaAs from this MBE system is in the 10^{14} cm^{-3} range. The higher mole fraction layers were doped with either Si (n type) or Be (p type) to roughly 10^{17} cm^{-3} , so that their electronic properties could be examined as well.^{8,9} For energies greater than the fundamental $\Gamma_{15V}-\Gamma_{1C}$ band gap, absorption due to free carriers and impurities is expected to be negligible^{10,11} at this doping level, hence the values of α thus obtained should be representative of the intrinsic materials.

Absorption samples were fabricated by first mounting specimens face down onto a clear glass slide using a transparent cyanoacrylate adhesive. The samples were then lapped to approximately 50 μm . After photolithographically defining 1-mm circular "windows," the samples were etched to their final thickness in a fast selective etch. This selective etch only affects $\text{Al}_x\text{Ga}_{1-x}\text{As}$ with $0 \leq x \leq 0.3$, so that samples with $x > 0.3$ were fabricated by merely etching to the epilayer, at which point transmitted light was clearly visible. The AIAs sample was loaded into the inert He atmosphere of the cryostat within three minutes of fabrication to prevent oxidation. Heterostruc-

tures with $x < 0.3$ were grown with a very thin etch-stop layer between the $\text{Al}_x\text{Ga}_{1-x}\text{As}$ epilayer and the substrate. This etch stop was readily removed with a dilute HCl solution, leaving only the $\text{Al}_x\text{Ga}_{1-x}\text{Al}$ epilayer. All samples were carefully examined with an optical microscope to ensure that no cracks or pinholes were present.

The higher mole fraction ($x \geq 0.39$) epilayers were capped with a thin n -GaAs layer during epitaxial growth, the purpose of which was to prevent oxidation and to facilitate ohmic contact formation for the studies in Refs. 8 and 9. The optical density of this layer (as determined from the foregoing study), the thickness of which was typically less than 5% of that of the $\text{Al}_x\text{Ga}_{1-x}\text{As}$ layer, was later subtracted from the total measured optical density as follows: let T' and D' be the measured transmission and optical density, respectively. Now

$$D' \equiv -\log_{10} T',$$

$$D_{\text{Al}_x\text{Ga}_{1-x}\text{As}} = D' - D_{\text{GaAs}},$$

so that finally $T = 10^{-D}$ for the $\text{Al}_x\text{Ga}_{1-x}\text{As}$ layer. While it is true that this approach ignores reflections from the GaAs/AlGaAs interface, these reflections are in fact negligible, since the two materials have very similar indexes of refraction. Using published data¹² for $h\nu = 1.74$ eV and $x = 0.38$, for example, and with $k \ll n$, the reflectance $R = (n_2 - n_1)^2 / (n_2 + n_1)^2 = 1.1 \times 10^{-3}$. This method has been employed by previous authors in the analysis of absorption in GaAs/AlGaAs heterolayers as well.¹³

To account for reflection from the glass slide, 100% transmission was measured with an identical glass slide between the light source and the monochromator. The transmission T is then merely the quotient of the light transmitted through the sample and that transmitted through the glass slide. As a control, a second sample was fabricated from one of the wafers ($x = 0.39$) by mounting the sample to a glass substrate with white paraffin rather than the adhesive, and subsequently dismounting it prior to measurement such that the transmission was measured through the epilayer alone. In this instance, of course, 100% transmission was gauged without a glass slide between the light source and the monochromator. The resultant absorption coefficient curve agreed within experimental error (on the order of 10%) with that obtained from the sample permanently mounted as described above.

During both photoluminescence and optical transmission measurements, the samples were cooled to below 4 K in a Janis optical cryostat. A tungsten-filament lamp served as a broadband source for transmission. Photoluminescence was excited with the 5682 Å line of a Kr^+ ion laser. In both instances, the detected signal was focused onto the entrance slit of a 1.26-m focal length Spex grating monochromator. During transmission measurements, monochromator slits were narrowed and protected with neutral density filters due to the high intensity of the transmitted light. The detector employed throughout the experiment was a thermoelectrically cooled GaAs photocathode photomultiplier used in standard synchronous mode.

RESULTS AND DISCUSSION

For a uniform epilayer of material of thickness d with refractive index $n - ik$, reflectivity R , and absorption coefficient α , the transmission is given by

$$T = \frac{(1-R)^2 e^{-\alpha d}}{1 - R^2 e^{-2\alpha d}}, \quad (1)$$

where

$$R = \frac{(n-1)^2}{(n+1)^2}.$$

This expression assumes $k \ll n^2$ and ignores the effect of interference, which was not observed above the direct band gap, although strong interference was invariably observed below the optical (direct) band gap. Thus the expression used to analyze the data is (1), where α is derived from T as determined directly from the transmission data. For the purpose of analysis, values of R were obtained by setting $\alpha d = 0$ just below the band gap. These values were generally near 0.3, in agreement with previously reported reflectivity measurements.¹¹ The slight increase in R with photon energy has been ignored, as its effect is much less than the experimental error.

The absorption coefficient spectra are plotted as a function of incident photon energy $h\nu$ and alloy composition x in Fig. 1. Effects due to discrete excitons have been subtracted out as they will be discussed in detail shortly, and would only serve to obscure the curves on this energy scale. The shapes of these curves correlate closely with recent theoretical calculations¹⁴ taking into account the effect of alloy disorder by employing the coherent-potential approximation (CPA) rather than the virtual crystal approximation (VCA) for the crystal potential. This theory predicts the onset of absorption coefficient tailing below the direct band gap for $\alpha \geq 2 \times 10^3 \text{ cm}^{-1}$ at an alloy composition just above the direct- and/or indirect-band-gap transition. This phenomenon is observed in all of the

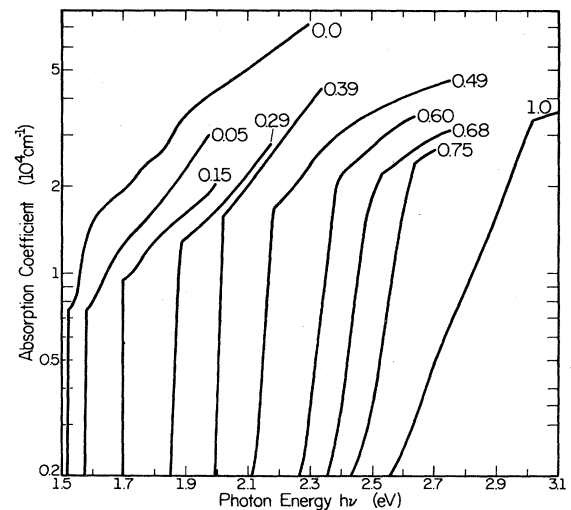


FIG. 1. Experimental absorption coefficient spectra for $\text{Al}_x\text{Ga}_{1-x}\text{As}$ with $0 \leq x \leq 1$.

indirect-band-gap epilayers, with the tail extending farther below the optical gap as x increases. The increase stems from the growing separation between the Γ minimum and the X and L minima, and also in part from the increase in background impurity concentration with x .

One effect that the above CPA model does not take into account, however, is the increase in the threshold value of α (at the optical band gap) with x . Note that simple theory predicts¹⁵ that near the band gap, the absorption coefficient $\alpha(x) = A(x)(h\nu - E_g)^{1/2}$, where the constant $A(x)$ depends on the exciton effective mass $m^*(x)$ and the dielectric constant $\epsilon(x)$. Extending the treatment of Ref. 4, a simple theoretical expression can be obtained for the normalized threshold absorption coefficient

$$\frac{\alpha_{th}(x)}{\alpha_{th}(0)} = \frac{[m^*(x)/m^*(0)]^{3/2}}{\epsilon(x)/\epsilon(0)}$$

This expression was employed using known values of $m^*(x)$ (Ref. 16) and $\epsilon(x)$ (Refs. 17 and 18) to generate the curve in Fig. 2, with the normalized exciton effective mass approximated by the normalized electron effective mass in the gamma valley. This approximation holds because the hole effective mass is significantly greater than the electron effective mass and displays a relatively weak x dependence. The data points were determined from threshold values in Fig. 1. For direct-band-gap alloys, α_{th} was taken at an energy just above the observed exciton structure. In the indirect region, α_{th} was read from the knee in the α curve, corresponding to the Γ minimum. Note the close fit to the theoretical curve over the entire alloy range, including the first datum from AlAs obtained in this manner. The energy of α_{th} gives the value of $\Gamma_{15V} - \Gamma_{1C}$ at 3 K for AlAs as 3.02 eV. This is quite consistent with the 300 K value of 3.1 eV determined from optical-absorption measurements.¹⁹ A greater than four-fold increase in α_{th} is observed as x varies from 0 to 1. Previous authors⁴ using the same techniques to obtain and

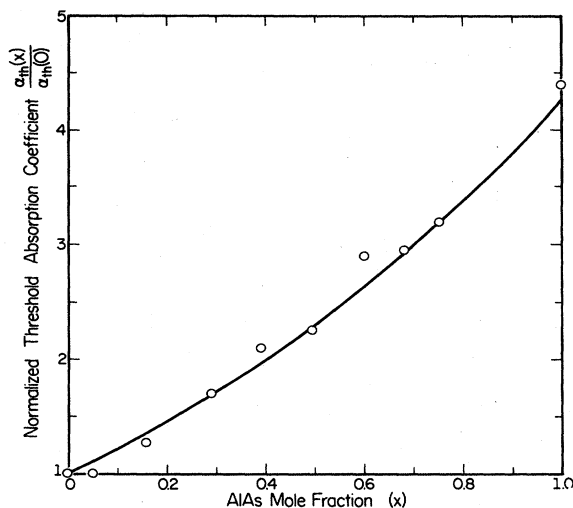


FIG. 2. Functional dependence of the normalized threshold absorption coefficient on $\text{Al}_x\text{Ga}_{1-x}\text{As}$ alloy composition. The open circles (\circ) represent experimental data, while the solid curve is theoretical.

analyze the data concerning this alloy system for $x \leq 0.87$ have presented curves showing only a twofold enhancement in α_{th} over the entire composition range. While the reason for this discrepancy is not clear, the present results concur much more closely with simple theory.

Having reviewed the general features of broadband optical absorption in the $\text{Al}_x\text{Ga}_{1-x}\text{As}$ alloy, the reader's attention is directed now towards the observed exciton features. Figure 3 depicts photoluminescence (solid curves) and transmission (dashed curves) spectra on the same wavelength scale for (a) $x=0$, (b) $x=0.05$, and (c) $x=0.35$; vertical scales are arbitrary in all cases. A detailed investigation of the emission (photoluminescence) spectra is still in progress, hence the present discussion will center on absorption features. First consider the GaAs spectra in Fig. 3(a). The emission spectrum displays the well-known spectral peaks^{20,21} commonly observed in GaAs. The three dominant exciton lines are the $n=1$ free-exciton (F,X) line at 1.5151 eV, the exciton bound to neutral donor (D^0,X) at 1.5140 eV, and the exciton bound to neutral acceptor (A^0,X) at 1.5123 eV. Four absorption lines are clearly visible in the transmission spectrum. The lowest in energy (rightmost) appears as a local minimum in the below-band-gap interference spectrum at 1.5139 eV, and can unambiguously be assigned to the (D^0,X) system. The reason that this peak appears while the acceptor is not seen in the transmission is the relatively large oscillator strength of the donor bound exciton. As photon energy increases, the next two features

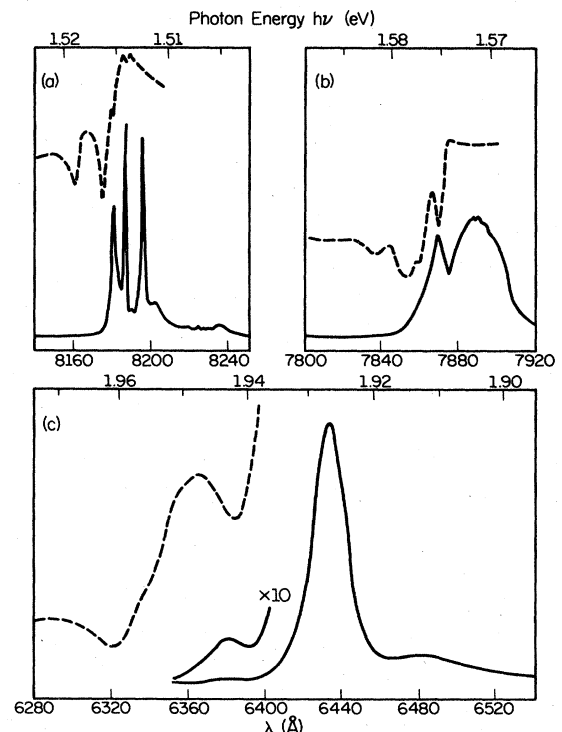


FIG. 3. Optical transmission (dashed curves) and photoluminescence (solid curves) spectra for $\text{Al}_x\text{Ga}_{1-x}\text{As}$ with (a) $x=0.00$, (b) $x=0.05$, and (c) $x=0.35$. All reveal near-band-gap excitonic transitions as described in the text.

are encountered at 1.5150 and 1.5160 eV. These are attributed to the lower and upper polariton branches of the $n=1$ (F,X), respectively. It has been verified experimentally that the transmission peak between the polariton branches is not an emission line excited by the high-intensity broadband light source. The true energy of the longitudinal free exciton (neglecting band parabolicity near $k=0$) must lie between these two; it is best given by the transmission peak separating them at 1.5152 eV. The highest energy line at 1.5182 eV is due to the $n=2$ (F,X). All of these spectral locations coincide within 0.1 MeV of accepted experimental values for these lines in emission^{20,21} and in absorption²² using a presumably more sensitive technique and high-purity epilayers as thick as 53.2 μm , which are not expected to show strong interference effects at wavelengths corresponding to the GaAs band gap, i.e., 0.82 μm . The close correlation of the absorption line energies with both present and previous data support the assumption that no significant strain was induced in the samples during the curing of the cyanoacrylate adhesive and subsequent cooling to superfluid helium temperatures.

Peak assignments in the $\text{Al}_x\text{Ga}_{1-x}\text{As}$ layers are analogous to the GaAs case. The transmission spectrum in Fig. 3(b), with $x=0.05$, displays the same features identified in GaAs: a bound exciton at the same energy as the dominant emission peak at 1.5755 eV, lower and upper polariton $n=1$ free-exciton branches at 1.5776 and 1.5788 eV, respectively, and an $n=2$ (F,X) line at 1.5817 eV. The $n=1$ (F,X) energy is taken to be 1.5777 eV. The $n=1$ (F,X) line does not appear in the emission spectrum of this sample, as is often the case even with high-purity GaAs under moderate excitation conditions. This is consistent with the relatively large magnitude of the bound-exciton absorption feature as compared to Fig. 3(a). This represents the first experimental report of polariton splitting of the free exciton in $\text{Al}_x\text{Ga}_{1-x}\text{As}$, or of any detailed exciton structure in optical transmission in this alloy system.

The $x=0.35$ epilayer transmission spectrum reveals two features. The lower energy line corresponds in energy to the highest energy emission line. Since this emission line is weak in comparison with the dominant (bound) exciton line, it is ascribed to the $n=1$ (F,X) system. Note that due to alloy transition broadening effects, no polariton splitting is observed, so that the $n=1$ (F,X) energy is derived from the relative transmission minimum at 1.9416 eV. The second (leftmost) absorption line occurs at 1.9610 eV, and is identified as the $n=2$ (F,X) since this is the only system observed at an energy greater than the $n=1$ (F,X) system in any sample.

Once the $n=1$ and 2 free-exciton energies have been obtained in this fashion, the binding energies can then be extracted. Baldereschi and Lipari have shown²³ that their model is applicable to this system. The expression for the free-exciton binding energy E_b given by this model is

$$E_b = 1.35(E_2 - E_1),$$

where E_1 and E_2 are the energetic position of the $n=1$ and 2 free excitons, respectively. Having calculated the exciton binding energies in this manner, the fundamental

energy gap at $\Gamma_{15V}-\Gamma_{1C}$ for direct-band-gap alloy compositions is simply given by

$$E_g = E_1 + E_b.$$

Applying the above treatment to the GaAs data yields $E_b = 4.0 \pm 0.3$ MeV, in agreement with the commonly accepted value.^{23,24} The value of $E_g = 1.5193 \pm 0.0003$ eV deduced from the present data agrees closely with that obtained by applying the same model to the data of Ref. 21, and also coincides with published values of E_g (Refs. 24–26) thus establishing the validity of the model. Assuming that effects introduced by the presence of aluminum in GaAs (such as local potential fluctuations) are small, the model has been extended to the $\text{Al}_x\text{Ga}_{1-x}\text{As}$ epilayers with $x \leq 0.43$. Free-exciton lines were not observed in the higher mole fraction samples. Once E_g is obtained, accurate values for the alloy composition x can be determined using the expression from Ref. 16 extrapolated to 0 K

$$E_g(x) = 1.424 + 1.247x + \Delta(x),$$

where $\Delta(x) = 0.0940 - x(0.0940 - 0.0750)$ is the extrapolation term. The two numbers in the difference comprising the coefficient of x represent the total change in E_g between 300 and 0 K for GaAs and AlAs, respectively. It should be pointed out that such a linear approximation for $E_g(x)$ is only reliable in the direct-band-gap alloy composition regime, where the virtual approximation for the crystal potential $V(x) = (1-x)V_{\text{GaAs}} + xV_{\text{AlAs}}$ holds reasonably well¹⁴ for the determination of the band structure. At higher mole fractions $x > 0.45$, a quadratic term

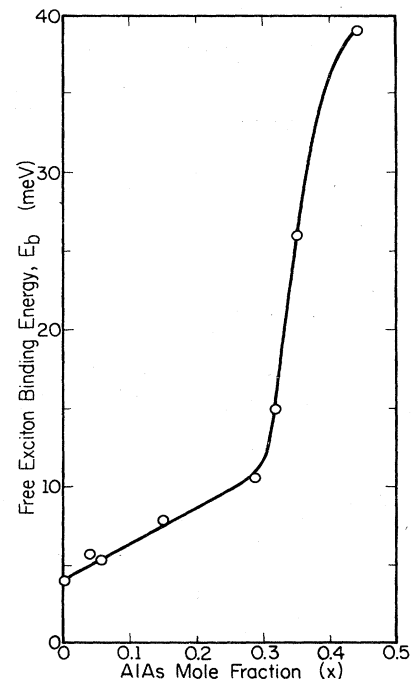


FIG. 4. The behavior of the binding energy of the free exciton in $\text{Al}_x\text{Ga}_{1-x}\text{As}$ as a function of x . Note the sharp, donor-like increase for $x \geq 0.25$.

takes into account bowing¹⁶ in the $E_g(x)$ relation to first order. The above treatment provides an accurate method for determining alloy compositions of high-purity direct-band-gap $\text{Al}_x\text{Ga}_{1-x}\text{As}$ epilayers from optical transmission measurements.

The free-exciton binding energies E_b in $\text{Al}_x\text{Ga}_{1-x}\text{As}$ are plotted in Fig. 4. It should be noted that the uncertainty in the binding of energy increases with x due to transition broadening; the uncertainty at $x=0.43$ is approximately 10%. For $x \leq 0.25$, the energies display a nearly linear dependence on alloy composition, rising to 10 MeV at $x=0.3$. Beyond this mole fraction, however, the binding energy exhibits a dramatic increase with x up to $x=0.43$, beyond which data are not yet available. The observed increase stems from a superlinear increase in the free-exciton effective mass that comes about as a result of multivalley effects. This behavior is similar to the composition dependence of the activation energies of various donors that have been studied.^{27-32,8} The similarity is easily understood; both the donor and the free exciton are systems involving a relatively large positively charged mass and an electron. Aside from the mass of the positive charge, the most significant difference between these two systems is the degeneracy of the valence band in the free-exciton case. At higher mole fractions, one would expect E_b to display a maximum near $x=0.45$, then decrease monotonically with x throughout the remainder of the alloy range. This is the first experimental observation of superlinear exciton binding-energy alloy dependence in $\text{Al}_x\text{Ga}_{1-x}\text{As}$. More work is needed to completely determine the x dependence of the binding energy in the indirect-band-gap regime.

In summary, a complete experimental study of low-temperature optical absorption in the $\text{Al}_x\text{Ga}_{1-x}\text{As}$ com-

pound semiconductor alloy system over the entire alloy composition range has been performed. The first experimental absorption coefficient curve for all AlAs covering energies greater than 2.7 eV is presented, including the $\Gamma_{15V}-\Gamma_{1C}$ direct-energy-gap spectral region. The energy of the optical gap of AlAs obtained at 3 K is 3.02 eV, which is consistent with other observations. The compositional dependence of the threshold α values of the absorption coefficient spectra concurs well with present theoretical predictions, and is significantly different from previous reports. Also, the first observation of detailed excitonic fine structure in transmission spectra of direct-band-gap $\text{Al}_x\text{Ga}_{1-x}\text{As}$ epilayers is reported, including features associated with bound excitons, $n=2$ free excitons, and the upper and lower polariton branches of the $n=1$ free exciton. This structure provides vital information concerning basic properties of the semiconductor, including the free-exciton binding energy, the $\Gamma_{15V}-\Gamma_{1C}$ direct energy gap, and hence the exact alloy composition x . Free-exciton binding energies were found to increase sharply for $x > 0.25$, much as donor activation energies increase near the direct- to indirect-band-gap transition region due to multivalley contributions to the effective mass.

ACKNOWLEDGMENTS

The authors wish to thank Dr. M. V. Klein for discussions and for access to this optical laboratory and Dr. Y. C. Chang for discussions concerning his recent theoretical work. D. Fu provided assistance in sample preparation. This work is supported by the Air Force Office of Scientific Research.

- ¹Zh. I. Alferov *et al.*, *Zh. Tekh. Fiz.* **48**, 809 (1978) [*Sov. Phys.—Tech. Phys.* **23**, 476 (1978)].
- ²T. E. Bell, *IEEE Spectrum* **20**, 38 (1983).
- ³G. Lucovsky and P. H. Cholet, *J. Opt. Soc. Am.* **50**, 979 (1960).
- ⁴B. Monemar, K. K. Shih, and G. D. Pettit, *J. Appl. Phys.* **47**, 2604 (1976).
- ⁵M. R. Lorenz, R. Chicotka, and G. D. Pettit, *Solid State Commun.* **8**, 693 (1970).
- ⁶T. J. Drummond, H. Morkoç, and A. Y. Cho, *J. Cryst. Growth* **56**, 449 (1982).
- ⁷T. Henderson, W. Kopp, R. Fischer, J. Klem, H. Morkoç, L. P. Erickson, and P. W. Palmberg, *Rev. Sci. Instrum.* **55**, 1763 (1984).
- ⁸N. Chand, T. Henderson, J. Klem, W. T. Masselink, R. Fischer, Yia-Chung Chang, and H. Morkoç, *Phys. Rev. B* **30**, 4481 (1984).
- ⁹N. Chand, R. Fischer, J. Klem, T. Henderson, P. Pearah, W. T. Masselink, Y. C. Chang, and H. Morkoç, *J. Vac. Sci. Technol. B* **3**, 644 (1985).
- ¹⁰H. Y. Fan, *Semiconductors and Semimetals*, edited by R. K. Willardson and B. C. Beer (Academic, New York, 1967), Vol. 3, p. 409.
- ¹¹J. I. Pankove, *Optical Processes in Semiconductors* (Dover, New York, 1975), Chap. 3.
- ¹²H. C. Casey, Jr., D. D. Sell, and M. B. Panish, *Appl. Phys. Lett.* **24**, 63 (1974).
- ¹³D. D. Sell and H. C. Casey, Jr., *J. Appl. Phys.* **45**, 800 (1974).
- ¹⁴D. Z. Y. Ting and Y. C. Chang, *Phys. Rev. B* **30**, 3309 (1984).
- ¹⁵R. J. Elliot, *Phys. Rev.* **108**, 1384 (1957).
- ¹⁶H. C. Casey, Jr., *J. Appl. Phys.* **49**, 3684 (1978).
- ¹⁷I. Strzalkowski, S. Joshi, and C. R. Crowell, *Appl. Phys. Lett.* **28**, 350 (1976).
- ¹⁸R. E. Fern and A. Onton, *J. Appl. Phys.* **42**, 3499 (1971).
- ¹⁹B. Monemar, *Solid State Commun.* **8**, 2121 (1970).
- ²⁰D. D. Sell, S. E. Stokowski, R. Gingte, and J. V. DiLorenzo, *Phys. Rev. B* **7**, 4568 (1972).
- ²¹U. Heim and P. Hiesinger, *Phys. Status Solidi B* **66**, 461 (1974).
- ²²D. E. Hill, *Solid State Commun.* **11**, 1187 (1972).
- ²³A. Baldereschi and N. O. Lipari, *Phys. Rev. B* **8**, 2697 (1973).
- ²⁴D. D. Sell, *Phys. Rev. B* **6**, 3750 (1972).
- ²⁵D. Bimberg and W. Schairer, *Phys. Rev. Lett.* **28**, 442 (1972).
- ²⁶M. D. Sturge, *Phys. Rev.* **127**, 768 (1972).
- ²⁷A. J. Spring Thorpe, F. D. King, and A. Becke, *J. Electron. Mater.* **4**, 101 (1975).
- ²⁸R. J. Nelson, *Appl. Phys. Lett.* **31**, 351 (1977).

²⁹M. Ayabe, Y. Mori, and M. Watanabe, *Jpn. J. Appl. Phys.* **20**, L55 (1981).

³⁰D. V. Lang, R. A. Logan, and M. Jaros, *Phys. Rev. B* **19**, 1015 (1979).

³¹J. J. Yang, L. A. Mandy, and W. I. Simpson, *Appl. Phys. Lett.* **40**, 244 (1982).

³²N. Lifshitz, A. Jayaraman, and R. A. Logan, *Phys. Rev. B* **21**, 670 (1980).